



จุฬาลงกรณ์มหาวิทยาลัย
ทุนวิจัย
กองทุนรัชดาภิเษกสมโภช

รายงานวิจัย

การสังเคราะห์ฟิล์มบางพิเศษของซิลิกา
โดยใช้เทคนิคแอตโมเชลล์

โดย

จินตนา สายวรรณ

กันยายน ๒๕๕๖

จุฬ
ปค 15
012134

จุฬาลงกรณ์มหาวิทยาลัย

ทุนวิจัย

กองทุนรัชดาภิเษกสมโภช



รายงานผลงานวิจัย

การสังเคราะห์ฟิล์มบางพิเศษของซิลิกาโดยใช้เทคนิคแอดไมเซลล์
(Mesostructural Ultra Thin Silica Film Formation through
Admicellar Technique)

โดย

สถาบันวิทยบริการ
จุฬาลงกรณ์มหาวิทยาลัย
รองศาสตราจารย์ ดร. จินตนา สายวรรณ

กันยายน 2546

Acknowledgements

The author would like to thank associate Professor John H. O'Haver and his atomic force microscope (AFM) group at the Chemical Engineering Department of the University of Mississippi-Oxford, USA for AFM training and facility. Also, the thanks go to the Rachadapiseksompoch Fund of Chulalongkorn University for the research support. Without their help and support, the work has not been possible.



สถาบันวิทยบริการ
จุฬาลงกรณ์มหาวิทยาลัย

เลขหมู่	คท ฟ๓ 15
เลขทะเบียน	012134
วัน, เดือน, ปี	10 มี.ค. 48

ชื่อโครงการวิจัย การสังเคราะห์ฟิล์มบางพิเศษของซิลิกาโดยใช้เทคนิคแอตไมเซลล์

ชื่อผู้วิจัย รองศาสตราจารย์ ดร. จินตนา สายวรรณ

เดือนและปีที่ทำวิจัยเสร็จ กันยายน 2546



บทคัดย่อ

การศึกษาการเกิดฟิล์มของซิลิกาจากการละลายของสารก่อซิลิกาอนินทรีย์ เตตรา-บิวทอกซีไฮโดรเจน (ทีบีไอเอส) และเตตราเอทิล ออโทซิลิเกต (ทีไอเอส) ในแอตไมเซลล์พอลิเมอโรเซชันเกิดขึ้นโดยใช้เซอร์แฟคแทนท์เทมเพลตของซิลิโคไตรเมทิลแอมโมเนียมโบรไมด์ (ซีแทบ) ที่ความเข้มข้น 700 ไมโครโมลาร์ และออกซิลฟีนอลเอทอกซิลเลท หรือไตรตอน เอ็กซ์-100 ความเข้มข้น 200 ไมโครโมลาร์ เพื่อละลายทีบีไอเอสและทีไอเอส ตามลำดับ ภาพจากอะตอมมิกฟอร์ซไมโครสโคปี (เอเอฟเอ็ม) ในระบบของทีบีไอเอส/ซีแทบ เป็นไฟเบอร์ โครงวงกลมและชั้นแบนราบปกคลุมพื้นที่บนผิวหน้าของไมกาเพิ่มขึ้น เมื่อเพิ่มความเข้มข้นของทีบีไอเอส และเกิดการแยกของเฟสขึ้นที่ความเข้มข้นต่ำ ส่วนที่ความเข้มข้นสูงไม่เกิดการแยกเฟสแต่ฟิล์มของซิลิกาแบนราบหรือเป็นหลายชั้นซึ่งเกิดขึ้นจากการละลายของซิลิเกตแอนอิกอนหรือโอลิโกเมอร์ที่อินเทอร์เฟซของแอตไมเซลล์กับสารละลาย สำหรับระบบที่ไอเอส/ไตรตอน เอ็กซ์-100 พบว่าภาพของผิวหน้าไมกามีรูปร่างกลมเป็นเนื้อเดียวกัน แสดงว่าการละลายของทีไอเอสเกิดขึ้นที่อินเทอร์เฟซของแอตไมเซลล์กับน้ำ การเติมสไตรีนโมโนเมอร์และตัวริเริ่มปฏิกิริยา 2,2'-เอโซบิส(ไอโซบิวทีโรไนทริล (เอไอบีเอ็น) ช่วยเพิ่มการละลายของทีไอเอสอย่างมากที่ใจกลางของแอตไมเซลล์ของไตรตอน เอ็กซ์-100 ภาพผิวหน้าของฟิล์มที่เกิดขึ้น ขึ้นอยู่กับปริมาณความเข้มข้นของสไตรีนและทีไอเอส การเพิ่มความเข้มข้นของสไตรีนช่วยเสริมการเกิดเป็นคอมโพสิทฟิล์มซิลิกาเปลี่ยนโครงสร้างที่เป็นหย่อมให้เป็นเนื้อเดียวกันโดยสไตรีนที่สูงขึ้นช่วยให้ทีไอเอสเข้าไปในพอลิ-สไตรีนดีขึ้น และกั้นการเกิดอนุภาคซิลิกาเกาะบนผิวหน้าไมกาที่ความเข้มข้นของสไตรีนและทีไอเอสเท่ากับ 3 ไมโครโมลาร์

Project Title Mesostructural Ultra Thin Silica Film Formation through Admicellar
Technique

Name of the Investigator Associate Professor Chintana Saiwan

Year 2003

Abstract

Thin silica film formation from adsolubilization of inorganic silica precursors, tetra-n-butoxysilane (TBOS) and tetraethyl orthosilicate (TEOS) in admicellar polymerization were studied. Cetyltrimethylammonium bromide (CTAB) at 700 μM and octyl phenol ethoxylate or Triton X-100 at 200 μM were used as surfactant templates for adsolubilizes TBOS and TEOS respectively. For the TBOS/CTAB system, the atomic force microscopy (AFM) topographic images showed fibers, hemispheres and flat layers existing along with increase of surface coverage on the mica surface as the TBOS feed concentration was increased. The results showed phase separation at low TBOS concentration. At high TBOS concentration, where there was no phase separation, the silica film was flat layer or multi-layer occurring from solubilization of silicate anion or oligomers at the admicelle-aqueous solution interface. For the TEOS/ triton X-100 system, the surface morphology on the mica surface exhibited the thin homogeneous globular-shaped features implying solubilization of TEOS at the admicelle-water interface. Addition of styrene monomer and 2,2'-azobisisobutyronitrile (AIBN) initiator promoted adsolubilization of TEOS significantly in admicellar core of triton X-100. The surface morphology of the film depended on the amount of styrene and TEOS feed concentrations. As the styrene concentration increases, the periodic structures become more homogeneous. Higher concentration of styrene assisted the incorporation of TEOS in the polystyrene and inhibited the formation of silica particles on the surface. At 3 μM styrene and TEOS concentrations, styrene and TEOS synergistically fabricate the composite silica film with high coverage density.

Table of Contents

Acknowledgements	i
Abstracts	ii
Table of Contents	iv
Chapter 1 Introduction	1
Chapter 2 Background and Literature Review	4
2.1 Adsorption of Surfactant on the Solid Oxide Surface	4
2.2 Sol-Gel Reaction (Inorganic Polymerization) of Alkoxysilane and Organic-Inorganic Hybridization with Polystyrene	6
2.3 Admicellar Polymerization	7
2.4 Atomic Force Microscopy	11
2.4.1 The Principle of Atomic Force Microscopy (AFM): Contact Mode	11
2.4.2 Force-Versus-Separation Curve	11
2.5 Muscovite Mica	14
Chapter 3 Experimental	15
3.1 Materials	15
3.2 Atomic Force Microscopy	15
3.2.1 Contact Mode (sample in an aqueous solution)	16
3.2.2 Tapping Mode (sample in air)	16
3.3 Film Preparations and Studies	16
3.3.1 Silica Film Formations in CTAB System	16
3.3.1.1 Adsorption of TBOS (without CTAB)	16
3.3.1.2 Admicellar Polymerization of TBOS	17

3.3.2 Silica Film Formations in Titron X-100/TEOS/Styrene-AIBN System	18
3.3.2.1 Adsorption of TEOS	18
3.3.2.2 Polystyrene Film Formation	18
3.3.2.3 Admicellar Polymerization of TEOS/ Styrene-AIBN	19
Chapter 4 Results and Discussion	20
4.1 Silica Film Formation in CTAB/TBOS System	20
4.1.1 The Existence and Structure of CTAB Admicelles on Mica	20
4.1.2 Adsorption of TBOS (without CTAB)	23
4.1.3 Admicellar Polymerization of TBOS	25
4.1.3.1 Adsolubilization and Film Characterization	25
4.2 Silica Film Formation in Triton X-100/TEOS-Styrene-AIBN System	28
4.2.1 Adsorption of TEOS	28
4.2.2 Polystyrene Film Formation	29
4.2.3 Admicellar Polymerization of TEOS/ Styrene-AIBN	31
Chapter 5 Conclusions	35
Recommendations	36
Comments and Remarks	37
References	38

Chapter 1



Introduction

Admicellar polymerization, polymerization of monomers solubilized in adsorbed surfactant aggregates, is a proven method of ultra thin film fabrication [1]. These films may provide specific properties to the surfaces of substrates, e.g. gold nanorods, gold nanoparticles, iron oxide colloids, silver colloids, and titania particles. These surface-modified materials play very important roles in functionally specific surface coatings, catalysis, microextraction, and semiconductor fabrication.

In the studies of surfactant adsorption on a solid surface, a full understanding of the results is often hampered by unknown factors, i.e. surface heterogeneity, roughness and porosity [2]. Molecularly smooth surfaces, e.g. mica with atomically smooth surface and the well-defined structure of known ion exchange property, may be used to overcome these uncertainties. Kekicheff *et al.* studied the adsorption of cetyltrimethylammonium bromide (CTAB) on the mica surface at CTAB concentrations below its critical micelle concentration (CMC) using a surface force apparatus [2]. They suggested that the adsorption of CTA^+ cations lead to the formation of a hydrophobic, near-neutral surface at CTAB concentration of 0.005 CMC. At higher CTAB concentrations, a positive charge builds up as further CTA^+ cations adsorb, probably oriented with the polar group towards the water phase. This highly charged adsorbed layer is well-formed at a CTAB concentration of 0.5CMC. The structure of the admicelle (adsorbed aggregates) can be spherical, cylindrical, or flat, much the same as micelle behavior [3]. Similar in nature to a micelle, the admicelle is characterized by three regions [1, 4]. The outer region is the most polar, consists of the surfactant headgroups, and forms the admicelle-solution and admicelle-solid interfaces. The inner region is referred to as the core region. This region consists of the hydrocarbon chains and is nonpolar in nature. The region between the headgroups and the core is the palisade region. This region is intermediate in polarity, consists of the carbons near the headgroups, and is also characterized by water molecules that have penetrated the admicelle. Various studies have indicated that

organic solutes partition into the regions of the admicelle that possess similar polarity. Thus, alkanes or other nonpolar solutes partition primarily to the core region, while polar components partition to the palisade region and the headgroup region. This partitioning is usually called “adsolubilization”. If the partitioning solutes could be polymerized to form a polymer on the substrate, the process is referred to as “admicellar polymerization” [1]. To date the admicellar polymerization has only been used to fabricate organic films, e.g. polystyrene [5, 6], polypyrrole [7], poly(vinylpyrrolidone) [8], and poly(tetrafluoroethylene) [9] on hydrophilic surfaces.

Recently, Fisher [10] and Maeda [11] successfully encapsulated hydrolysable silanes, e.g. n-alkoxysilanes, using a mixed surfactant solution. The surfactant prevents the coalescence of the n-alkoxysilane emulsion particles by ionic repulsion between particles. Addition of a co-surfactant, usually moderately long chain alcohols, reduces the releasing of encapsulated n-alkoxysilane. Emulsions prepared by this process have shelf-stability exceeding 6 months. This implies that a surfactant monolayer encapsulating n-alkoxysilane efficiently retards the polymerization of n-alkoxysilane. This retardation provides significant benefits to the admicellar polymerization of the monomers being able to degrade in their solvent at an ambient condition since admicellar polymerization needs sufficient time for the solutes to initially partition. These findings raise the possibility of admicellar polymerization being used for inorganic monomers, e.g., n-alkoxysilane, which has not been examined to date. This work studied the use of admicellar polymerization to the formation of inorganic film.

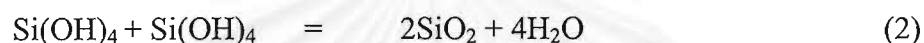
In our work, the admicellar polymerization of n-alkoxysilane inorganic monomer (precursor), we selected tetra-n-butoxysilane (TBOS), which has a moderately long alkyl chain and very low solubility in water [12] as the monomer. Its solubility (< 0.5 mg/L) implies a higher hydrophobicity and lower polarity than the n-alkoxysilane used in Fisher and Meada's work [10-11]. This solubility is also less than the solubility of styrene, which is well-known solute for admicellar polymerization. The polymerization of TBOS consists of 2 major reactions, i.e. hydrolysis and condensation as shown in equations (1) and (2), respectively. TBOS typically hydrolyzes in water very slowly (< 1 $\mu\text{mol/day}$ at 15-100 $^{\circ}\text{C}$ and pH 5-9) at TBOS initial concentrations of 10-100 mg/L [12]. It produces silanol and n-butanol as

major intermediate products. One silanol produced from the hydrolysis will react with another silanol forming solid silica and water as the final products - this reaction is called condensation.

Hydrolysis:



Condensation:



These properties of TBOS suggest that TBOS should be well encapsulated by surfactants in the admicelle due to two reasons, i.e., 1) similar polarity between TBOS and n-alkyl chain of surfactant and 2) longer partitioning time.

Atomic force microscopy (AFM) was used to examine the admicellar polymerization of TBOS adsorbed in CTAB admicelles for ultrathin silica film fabrication on a mica surface in an aqueous solution. The TBOS reactions on the mica surface were examined both with and without the presence of CTAB. System variables included TBOS feed concentration and reaction time. The film coverage was improved by changing the surface modifying solution to Triton X-100/styrene/AIBN/TEOS aqueous solutions for in-situ organic-inorganic hybridized polymerization to form polystyrene-doped silica film with higher film coverage density.

Chapter 2

Background and Literature Review

2.1 Adsorption of Surfactant on the Solid Oxide Surface

The adsorption of ionic surfactant onto an oppositely charged solid surface has been extensively studied. When a mineral oxide surface is brought into contact with an aqueous solution, the adsorption of H_3O^+ or OH^- ions from the solution onto the surface can cause variations in the surface charge. As the pH of the solution is lowered, the mineral oxide surface will usually become more positively charged (or less negatively charged) because of the adsorption of the H_3O^+ ions onto the surface, with the consequence of an increase in the adsorption of anionic surfactants and a decrease in the adsorption of cationic surfactants. The reverse is true when the pH of solution is raised.

Adsorption data have usually been presented as a log-log plot of the surfactant adsorption (amount of surfactant adsorbed per gram of adsorbent) versus the equilibrium concentration of the surfactant in a bulk solution. Adsorption isotherms usually take very much on characteristic shapes, depending upon the types of surfactant and substrate. Rosen described that adsorption isotherm of ionic surfactants onto an oppositely charged substrate and also sometimes – but not always – nonionic surfactants are typically S-shaped [13]. In case of nonionic surfactants, an ethoxylated nonylphenol, for example, will exhibit a similar isotherm on silica, but will not adsorb sufficiently strongly to show all the details of such an isotherm on alumina. Commonly, S-shaped isotherm can be divided into four regions as shown in Figure 2.1 and in each these regions corresponds to a different mechanism of surfactant adsorption.

In region I the surfactant adsorbs mainly by ion exchange and also the charge density, or potential at the Stern layer of the solid, remains almost constant. This region corresponds to very low adsorption densities and is sometimes referred to as the Henry's law region. The most important point is that there are no aggregates of

adsorbed surfactants in this region and may not even be detectable because it occurs at such low surfactant concentration.

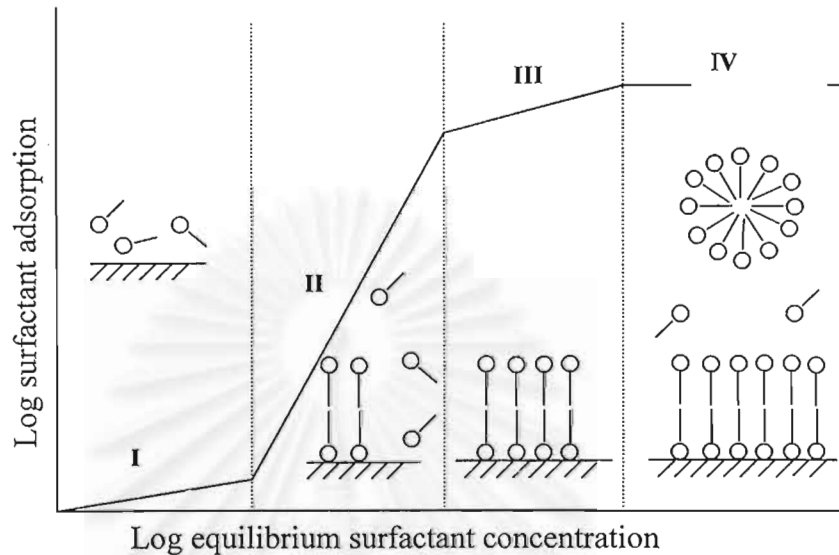


Figure 2.1: Adsorption isotherm for an ionic surfactant on an oppositely charged substrate [13].

In region II there is a marked increase in adsorption as the equilibrium concentration of surfactant increases. It is believed that this increase is caused by the interactions of the hydrophobic chains of oncoming surfactant ions with those of previously adsorbed surfactant and with themselves, which cause the adsorbed surfactants to form aggregates on the surface. This aggregation of the hydrophobic groups has been termed hemimicelle or admicelle depending upon whether the aggregates are viewed as monolayers or bilayers. The formation of these aggregates locally or patchwise at the interface is due to the heterogeneity of the surface. The original charged surface of the solid is neutralized by the adsorption of oppositely charged surfactant ions and eventually reverse, indicate the end of region II.

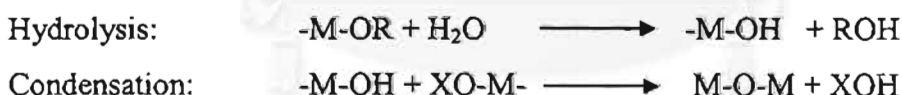
However, region III is characterized by a declined slope in the adsorption isotherm, not only because adsorption must overcome electrostatic repulsion between the oncoming ions and the identically charged head groups on the surfaces, but also because adsorption is now taking place on the more and more similarly charged surfaces. As the equilibrium concentration of surfactant further increases and

eventually approaches the critical micelle concentration (CMC), adsorption is usually completed. The beginning of constant adsorption marks the onset of region IV.

Region IV is referred to as the plateau adsorption region and in this region the surface concentration of surfactant has reached saturation. The adsorption does not increase while the equilibrium concentration of surfactant is raised above the CMC. Further addition of surfactants only contributes to the formation of additional micelles in the bulk solution. In most systems the transition of region III/region IV occurs near the CMC of the surfactants.

2.2 Sol-Gel Reaction (Inorganic Polymerization) of Alkoxysilane and Organic-Inorganic Hybridization with Polystyrene

Sol-gel is a method for preparing specialty metal oxide glasses and ceramics by hydrolyzing a chemical precursor or mixture of chemical precursors that pass sequentially through a solution state and a gel state before being dehydrated to glass or ceramic. The sol-gel reaction process generally involves the hydrolysis of metal alkoxides, followed by condensation reaction,



where X can be H or R (an alkyl group). Due to the immiscibility of orthosilicate with water, the reactions are generally carried out in a homogenizing solvent like alcohol.

Preparation of metal oxides by the sol-gel route proceeds through three basic steps: 1) partial hydrolysis of metal alkoxides to form reactive monomers, 2) the polycondensation of these monomers to form colloid-like oligomers (sol formation), and 3) additional hydrolysis to promote polymerization and cross-linking leading to a 3-dimensional matrix (gel formation). As polymerization and cross-linking progress, the viscosity of the sol gradually increases until the sol-gel transition point is reached. At this point the viscosity abruptly increases and gelation occurs. Further increases in the cross-linking are promoted by drying and other dehydration methods. Maximum density is achieved in a process called densification in which the isolated gel is heated

above its glass transition temperature. The densification rate and transition (sintering) temperature are influenced primarily by the morphology and composition of gel. Although presented sequentially, these reactions occur simultaneously after the initial processing stage [14].

The metal oxide also potentially can be in-structure hybrid with polymer, e.g., polystyrene, to improve the strength, thermal resistance, flexibility, film-substrate adhesion, and film spreading. To achieve these organic/metal oxide composite materials, the sol-gel method has to be combined with self-assembly through the surfactant template technique. Sol-gel polymerization of inorganic precursors within surface aggregates allows the creation of highly ordered organic-inorganic composites and the encapsulation of organic aggregates, preserving the morphologies of the flexible organic supramolecular structures [15]. The sol-gel process is essentially a physical chemistry route that allows one to obtain high-purity inorganic materials, with a wide variety forms, such as powders, fibers and films. It enables the introduction of organic elements into inorganic material without deteriorating their functionality. Accordingly, polystyrene was dispersed at a nano-meter level in the silica gel matrix. The properties of such hybrid networks strongly depend on various parameters such as the degree of phase dispersion, the relative amount of organic and inorganic components, type of catalyst, the molar ratio of water to silane, the reaction time, temperature and ionic strength as well as the molecular weight of polymer [16]. The final morphology of the nanohybrids is strongly dependent on the presence of the adsorbed surfactant, i.e., nonionic surfactant. Moreover, the surfactant not only enables the production of raspberry-like silica-polystyrene materials, but also ensures strong attachment of the polystyrene particles on the silica surface [17].

2.3 Admicellar Polymerization

Surfactants adsorbed at the solid-liquid interface can form aggregates that are much like micelles. These micelles can be used to solubilize organic molecules in the same manner that micelles are used [1]. This phenomenon has been explored as a way to deposit ultra-thin films on solid surfaces. The process may be described as occurring in 4 major steps as follows: 1) adsorption of surfactant to form two-

dimensional aggregates on solid surface acting as reactant storage, 2) incorporation or adsolubilization of reactant monomer or initiator into the aggregates, 3) polymerization of monomer and/or initiator within the aggregates, and 4) removal of surfactant as shown in Figure 2.2. The overall process, called admicellar polymerization, occurs below the CMC to minimize partitioning of monomer/initiator into micelles. The adsolubilization of monomer extensively depends on electrostatic contributions, monomer molecular volumes, the hydrophobic effect, and dipole interactions. To maximize adsolubilization, the monomer, which can be liquid or gas, should be insoluble or only slightly soluble in water so that only a very small fraction is present in the bulk phase. Potential monomers are such as styrene, pyrrole, acrylonitrile, and tetrafluoroethylene. These monomers were used to modify solid surfaces such as alumina, silica, mica, and glass fibers in order to obtain specific surface functionality, surface morphology, mechanical properties, electrical properties and other specific properties depending on the applications.

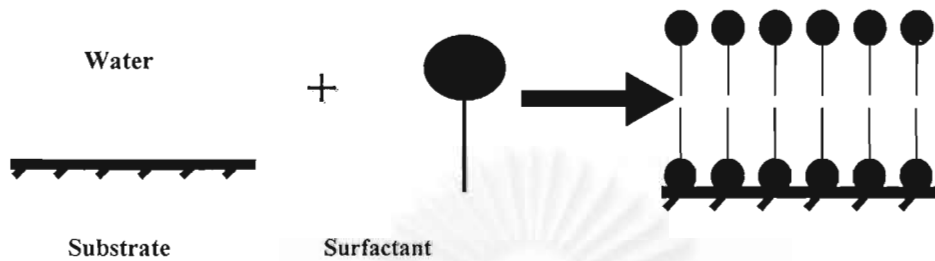
Step 1: Admicelle Formation

The formation of aggregate structures at solid/liquid interfaces to form bilayers (admicelles) through adsorption from an aqueous solution below critical micelle concentration is a well-known phenomena. The adsorption is accomplished through the use of suitable surfactant under appropriate system conditions. Two layers should form simultaneously on local patches of the surface, rather than by monolayer coverage preceding formation of the second layer [18]. To achieve admicelle formation, the adsorption of surfactants on solid substrates is controlled by several parameters including the electrochemical nature of the substrate, the pH of the solution, and the type of surfactant molecules. The most critical parameter to be manipulated is the solution pH [19].

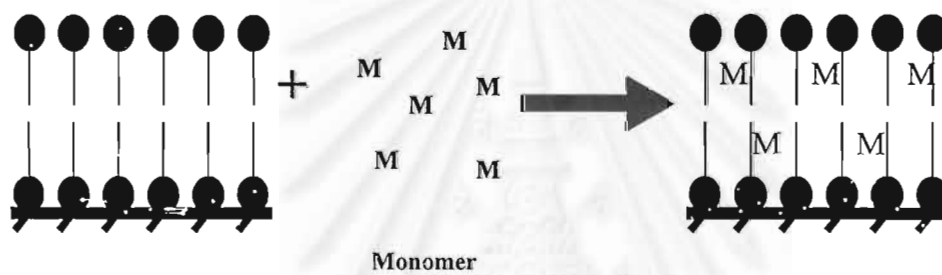
The solid oxide surface can be manipulated to possess either net positive or negative charge by adjusting the pH of the contacting the aqueous solution, and hydrogen and hydroxyl ions are potential determining ions for metal oxides. The pH at which the net charge on the surface is zero is called the point of zero charge (PZC). At pH values below the PZC, the surface becomes protonated and more positively charged; above the PZC, the surface is negatively charged. Consequently, anionic surfactants adsorb below the PZC and cationic surfactants above the PZC. As an

example, silica having $2 \leq \text{PZC} \leq 3$, will be negatively charged when the pH of the aqueous solution exceeds 3 [20].

Step 1.



Step 2.



Step 3.



Step 4.



“M”s represent solute molecules, monomers.

“P”s connected by lines represent polymer chains formed during the reaction.

Figure 2.2 The admicellar polymerization process for the formation of a thin polymer film.

Penfold *et al.* have previously shown that the adsorption of nonionic surfactants on silica is highly pH dependent [21]. At high pH (~9.0) desorption of nonionic surfactant occurs. The adsorption at pH 2.4 is significantly greater than that at pH 7.0. Decrease pH will decrease the surface charge density, which can be used to control the density of hydroxyl groups on the surface. Consequently, decrease the solution pH from 7.0 to 2.4 enhanced the adsorption. Exposure of the surface to solutions at low pH has produced a greater affinity of the nonionic surfactant for the surface than at higher pH. This is a clear evidence of the delicate nature of cooperative adsorption of nonionic surfactants at the hydrophilic silica.

Step 2: Monomer Adsolubilization

Adsolubilization is the surface analogue of solubilization, where aggregates of adsorbed surfactant play the role of micelles. Under conditions favorable for the formation of admicelles on solid surface in an aqueous supernatant, adsolubilization can be accomplished. Many organic monomers that are nearly insoluble in water will preferentially partition into the bilayer core because the admicelle interior is highly hydrophobic. The organic monomers that adsolubilize into the admicelle interior share the hydrophobic interaction with the amphiphile tails [18]. This process can occur after the formation of the admicelles, or concurrently with surfactant adsorption. It is convenient experimentally to dissolve the monomer, and often the initiator, in the surfactant feed solution prior to surfactant adsorption.

Step 3: In-Situ Polymerization of Adsolubilized Monomers

This is accomplished through the generation of free radicals capable of initiating the polymerization reaction. Once the polymerization reaction has been initiated and the monomer is being consumed in the admicelle, the monomer in the bulk solution can begin to re-equilibrate by diffusing into the admicelle. If the reaction continues for a sufficient length of time, virtually all monomers can be converted to polymer [1]. The conversion of monomer to polymer is a function of the reaction time [18].

Step 4: Surfactant Removal

The modified substrate is washed with water to remove excess surfactant layer in order to expose the polymer film. The powder is then dried in an oven at high

temperature to vaporize unreacted monomer and excess solvent. However, the temperature does not affect the properties of the polymer.

2.4 Atomic Force Microscopy

2.4.1 The Principle of Atomic Force Microscopy (AFM): Contact Mode [22].

The atomic force microscope, which was invented in 1986, permits resolution of individual atoms on both conducting and *insulating* surfaces. In this procedure, a flexible force-sensing cantilever stylus is scanned in a raster pattern over the surface of the sample. The force acting between the cantilever and the sample surface cause minute deflections of the cantilever, which are detected by optical means. The motion of the tip, or sometimes the sample, is achieved with a piezoelectric tube. During a scan, the force on the tip is held constant by the up-and-down motion of the tip, which then provides the topographic information. The advantage of the atomic force microscope is that it is applicable to non-conducting samples.

Figure 2.3 shows schematically the most common method of detecting the deflection of the cantilever holding the tip. A laser beam is reflected off a spot on the cantilever to a segmented photodiode that detects the motion of the probe. The output from the photodiode then controls the force applied to the tip so that it remains constant.

Figure 2.4 shows a common design of an AFM. The movement system is a tubular piezoelectric device that moves the sample in x, y, and z directions under the tip. The signal from the laser beam detector is then fed back into the sample piezoelectric transducer, which causes the sample to move up and down to maintain a constant force between the tip and the sample.

2.4.2 Force-Versus-Separation Curve

A force and separation curve can be recorded by holding, through sample-and-hold techniques, the tip at a particular x-y location far away from the surface. The tip is then driven in toward the surface at a rate, which is slow in comparison with the mechanical response of the system but fast in comparison with thermal drift.

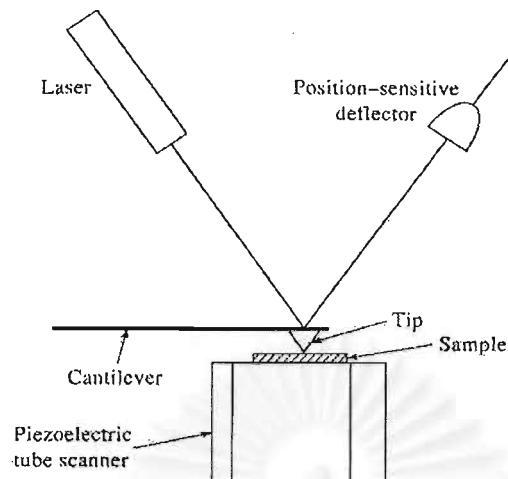


Figure 2.3: Side view of an optical beam deflection detector. Typically, the system is sensitive to 0.01 mm as the tip scans the sample surface.

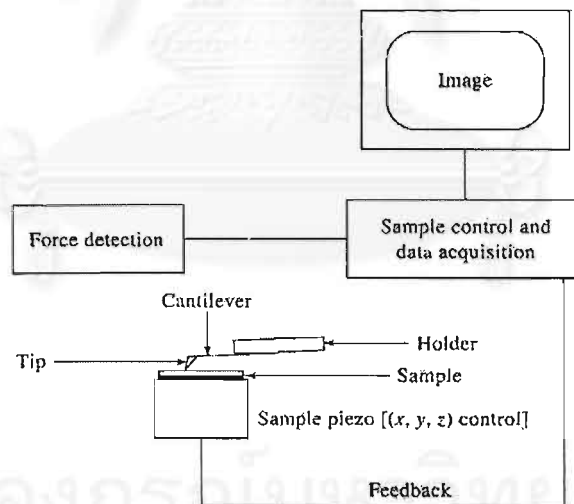


Figure 2.4: Typical design of an atomic force microscope.

The net force is sensed during the approach, contact, and retraction (drawing-off) parts of the cycle. An idealized curve is shown in Figure 2.5. Segment A-B reflects the attractive force regime; any structure in this part of the curve can be ascribed to the

functional dependence of the attractive forces on separation distance. These dependences are weak in comparison with those in other parts of the cycle. The relatively sudden drop at B toward C will generally occur due to meniscus force (operation in air) and/or adhesion forces. At, or near, point C, tip and surface will be in contact, and the slope of the segment C-D will be determined by the short-range repulsive force. If the surface is compliant due to finite hardness or if there are other kinds of relaxation at the point of contact, e.g., due to adsorbed molecular species, then there may be structure in the force-versus-separation curve at point C, and/or the slope C-D may be dependent on the material. The principal difference in the curve during retraction will be due to hysteretic effects around the points of making and breaking contact (B-C versus E-F). The making and breaking of the meniscus microbridge clearly will result in hysteresis, as will surface adhesion. As well, molecular rearrangements at the interface may be hysteretic. Typical dynamic ranges of force and separation can be up to 10^2 - 10^3 and 10^2 - 10^3 nm, respectively. A consequence of this discussion is the need to match the stiffness of the lever to the compliance of the system being investigated in order to extract maximum information.

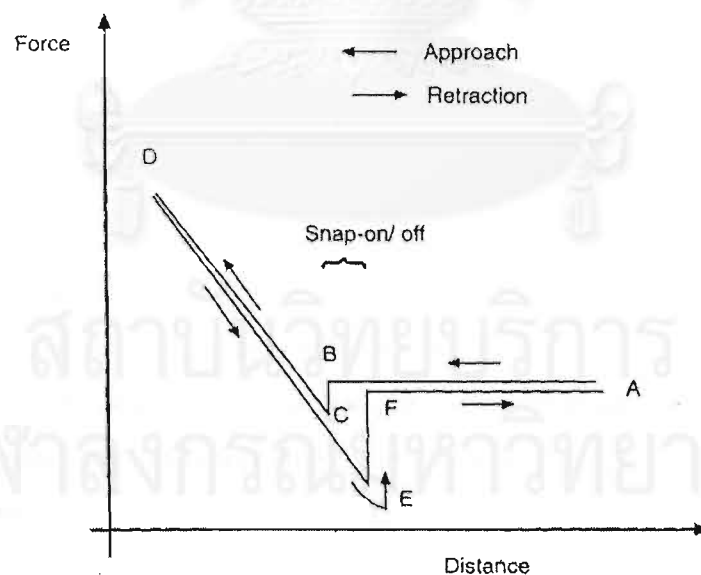


Figure 2.5: A schematic representation of AFM spectroscopic data, a force-versus-separation curve. Note the nearly horizontal sections represent the noncontact regime; the sloping straight line segments represent hard-sphere repulsive contact; and the hysteretic effects are due to snap-on and snap-off forces.

2.5 Muscovite Mica

The requirement of the flat surfaces for efficient AFM operation has concentrated most of the research on systems such as glass, quartz, silica, graphite, or mica substrate. Because it's well-defined structure and atomic smoothness of the surface, mica seemed to be a convenient model adsorbent to investigate via atomic force microscope.

Muscovite mica is a 2:1 layered silicate and its crystal structure consists of two tetrahedral silica sheets sandwiching an octahedral alumina sheet. On an average of one of four silicon atoms is replaced by aluminum, giving rise to localized negative surface charges that are more homogeneously distributed than those of montmorillonite. Therefore, muscovite is better suited to serve as substrate for such studies [23].

Narkiewicz-Michalek illustrated muscovite mica (ideal formula, $\text{KA}_2(\text{AlSi}_3\text{O}_{10})(\text{OH})_2$) as a layered aluminosilicate mineral consisting of 1 nm thick sheets that buildup an anisotropic structure [24]. The ionic bonds holding the sheets together in the crystal are weak compared with the covalent bonds within each sheet which facilitate cleavage between sheet planes. These molecularly smooth basal planes carry a large negative charge (1 charge/ 0.48 nm^2) because on the average one silicon atom out of four is replaced by aluminum atom. Because its well-defined structure and molecularly smooth surface, mica seemed to be a convenient model adsorbent to investigate that combined effect of surface heterogeneity and multisite occupancy adsorption.

In fact, Sakhalkar and Hirt have indicated the presence of inhomogeneity at the quartz surface that effect the uniformity of the adsorbed layer [19].

In a recent study, Cantrell and Ewing have been shown that muscovite mica is a popular choice for the study of interfacial phenomena because its almost perfect cleavage along the (001) plane removes the complexities introduced by roughness [25]. Furthermore, water has an affinity for the surface of mica. They also investigated thin film water on muscovite mica which is shown that water adsorbed to the (001) plane of muscovite mica has an infrared spectrum consistent with a bonding network that is more structured than that found in bulk water.

Chapter 3

Experimental

3.1 Materials

Cetyltrimethylammonium bromide (CTAB) greater than 99% purity (Sigma Chemical, USA) and octyl phenol ethoxylate or Triton X-100[®] with 100% purity (Union Carbide Chemicals and Plastics, USA) were used as surfactants. Tetra-n-butoxysilane (TBOS) greater than 95% (Gelest, USA), and tetraethyl Orthosilicate (TEOS) greater than 99% purity (Fluka, Switzerland) were used as inorganic monomers. Styrene with 99% purity (Sigma Chemical, USA) was used as an organic monomer. 2,2'-azobisisobutyronitrile (AIBN, 99% purity) (Aldrich, USA) was used as a polymerization initiator. Methanol (HPLC grade) was purchased from Fisher Scientific (USA). All chemicals were used as received. Mica discs (Ted Pella, California) with 9.9 mm in diameter were used as a hydrophilic substrate. They were freshly cleaved before use. De-ionized water obtained from a Barnstead E-pure water system with a resistivity of 18.3 M Ω .cm⁻¹ was used throughout this work.

3.2 Atomic Force Microscopy

The atomic force microscope, a MultiMode[™] scanning probe microscope (Digital Instruments, California) was equipped with a AS-130V ("J" vertical) piezoelectric scanner with maximum lateral and vertical scan ranges of 125 μ m \times 125 μ m and 5.0 μ m, respectively. The NanoScope IIIa software (Digital Instruments, USA) was used to capture and analyze images.

Surface images of samples in air were captured by the tapping mode and in aqueous solutions by the contact mode. The integral gain for each operation was set to 0.7-1.2 scan-rate at 1-5 Hz for both modes.

3.2.1 Contact Mode (sample in an aqueous solution)

A freshly cleaved mica disc was mounted on the top of the scanner. A fluid cell (Digital Instruments, USA) equipped with silicon nitride (Si_3N_4) probes (Model NP, Digital Instruments), was assembled covering a mica disc. The NP probe possesses length of 200 μm , nominal tip radii of 20-60 nm and manufactured-supplied spring constant of 0.06 N/m. A 0.3 mL of an aqueous solution shown in Table 1 is then injected into the fluid cell. The topographic and deflection images of the modified mica surface were operated at $22\pm 1^\circ\text{C}$ for all experiments. A measurement was done by sliding a tip probe across a mica surface, then a reflected laser light from the top of AFM cantilever is detected by a photodiode detector for further analyzing to provide a resulted topography.

3.2.2 Tapping Mode (sample in air)

The tapping mode was used to image the surface aggregates of dried silica film on mica surfaces in an ambient environment. A surface-modified mica disc was mounted onto the top of the scanner. A tapping mode etched silicon probe (Model TESP, Digital Instruments) possesses supplier-supplied spring constants of 20-100 N/m, nominal tip radii of 5-10 nm, and resonance frequencies of 200-400 kHz. The silicon probe was assembled with its holder and then the holder is put to cover the mica disc. The AFM was performed and the topographic and phase images were captured simultaneously while the temperature was kept at $22\pm 1^\circ\text{C}$ for all experiments. The operating relative humidity monitored by a humidity probe (Cole-Parmer Instrument) was not controlled but within 10 to 30%.

3.3 **Film Preparations and Studies**

3.3.1 Silica Film Formations in CTAB System

3.3.1.1 Adsorption of TBOS (without CTAB)

The adsorption of TBOS and its nucleation on mica surface without CTAB was used as a reference. A 0.266 μM TBOS aqueous solution (solution No. 1 in Table 1) clearly showed TBOS adsorption/nucleation. The phenomena were examined in the aqueous solution only approximately 3 hours due to solvent evaporation during

imaging. For long reaction time, the TBOS adsorption on mica surface was conducted in a glass vial containing the reactant solution. After the desired time had elapsed, the surface-modified mica was rinsed with de-ionized water for 5 minutes followed by methanol for 5 minutes, and then dried in a desiccator for 24 hours. Tapping mode AFM was then used to image the dried surface in air.

Table 1. Composition of the studied aqueous solution.

Solution No.	CTAB (μM)	TBOS (μM)
1	0	0.266
2	700	0
3	700	1.31
4	700	0.266
5	700	0.0266

Force-versus-separation curve to measure a true thickness of surface structure was performed in contact mode by moving the AFM tip probe from the position being far away from a mica surface downward to a mica surface and then drawing the tip upward to a beginning position again. The forces between the tip probe and the mica surface were constructed against the separation distances between the tip probe and a mica surface [26]. The experiment was performed in the CTAB concentration of 700 μM and in the absence of TBOS (solution No. 2).

3.3.1.2 Admicellar Polymerization of TBOS

The admicellar polymerization process was performed with starting solutions No. 2 to 5. The methodology is the same as that performed for TBOS adsorption study. Admicellar polymerization consists of 4 major steps as follows: 1) admicellization (adsorption of surfactant admicelles), 2) adsolubilization, 3) polymerization and 4) surfactant removal [1, 5, 6, 7, 8]. Our studies and methodologies will follow these steps.

Step 1: Surfactant adsorption was conducted in a 700 μM CTAB aqueous solution (solution No. 2) which is below the CMC of CTAB (920 μM) [13] but near

the plateau adsorption for CTAB on mica [14]. The admicelles at this concentration were observed by contact mode AFM in an aqueous solution after equilibration for 3 hours.

Step 2 and 3: The adsolubilization and polymerization of TBOS in the CTAB admicelles were performed simultaneously because TBOS is exposed to water during both steps. With the CTAB concentration fixed at 700 μM , the TBOS concentrations were set at 1.31, 0.266 and 0.0266 μM , as shown in Table 1. For short reaction times (< 3 hours), the images of surface aggregates in the aqueous solution were captured by the contact mode AFM starting immediately after injecting solutions No.3 or 4 or 5 onto mica surface in a fluid cell. For long reaction times, the admicellar polymerization was conducted in a glass vial containing solutions No. 3 or 4 or 5 before imaging.

Step 4: After desired time, the removal of residual CTAB on the surface-modified mica was performed by rinsing the surface with de-ionized water 5 minutes followed by methanol for 5 minutes. The surface-modified mica was then dried in a desiccator at ambient temperature for 24 hours before imaging by tapping mode AFM in air.

3.3.2 Silica Film Formation in Triton X-100/TEOS/Styrene-AIBN System

3.3.2.1 Adsorption of TEOS

Freshly cleaved mica was equilibrated in de-ionized water or surfactant solution for 24 hours before it was used. The triton X-100 concentration in an aqueous solution was 0.2 mM where at this concentration, triton X-100 is adsorbed as two dimensional aggregates, admicelles [27]. The cmc value of triton X-100 in an aqueous solution is 0.23 mM. Then the mica was immersed into the freshly prepared TEOS solution (3.0 μM) to equilibrate for 2 days. After that mica was washed with methanol and de-ionized water and was left to dry in a dessicator for at least 1 day under ambient condition.

3.3.2.2 Polystyrene Film Formation

The solution of styrene monomer (3 μM) and AIBN (0.5 μM) was prepared in 0.2 mM of triton X-100 aqueous solution. Amount of AIBN used was in the ratio of 1

mole of AIBN to 6 mole of styrene. Freshly cleaved mica was immersed in the solution and equilibrated for 2 days. Polymerization was conducted at 80°C in a water bath for 2 hours. The as-synthesized formed polystyrene on mica was washed with methanol and de-ionized water and was left to dry in a dessicator for at least 1 day under ambient condition.

3.3.2.3 Admicellar Polymerization of TEOS/ Styrene-AIBN

The styrene monomer (0.3 and 3.0 μM) and AIBN and mica in 0.2 mM of triton X-100 aqueous solution was prepared and equilibrated for 2 days as previously described. Amount of AIBN used was in the ratio of 1 mole of AIBN to 6 mole of styrene. Then, TEOS (0.3 and 3.0 μM) was added to the solution and allowed to equilibrate for another 2 days. Finally, polymerization was conducted at 80°C in a water bath for 2 hours. The as-synthesized polystyrene/silica composite film on mica was washed with methanol and de-ionized water and was left to dry in a dessicator for at least 1 day under ambient condition.



Chapter 4

Results and Discussion

4.1 Silica Film Formation in CTAB/TBOS System

4.1.1 The Existence and Structure of CTAB Admicelles on Mica

According to our main objective, we aimed to synthesize an ultra thin silica film on a mica surface by an admicellar polymerization of tetra-n-butoxysilane (TBOS) adsorbilizing in cetyltrimethylammonium bromide (CTAB) admicelles in an aqueous solution. The admicellar polymerization is generally performed in an aqueous surfactant solution below CMC to avoid a competitive adsorbilization and polymerization of TBOS in micelles. As known, the CMC of CTAB is 920 μM . Therefore, we selected a CTAB concentration of 700 μM (80% CMC) in all experiments.

To make sure that the selected concentration provided CTAB admicelles on mica surface, the surface topography by a contact mode of AFM was utilized to characterize the surface structure of the modified mica surface directly under the CTAB aqueous solution when no TBOS was added and 3 hours equilibration. The result is shown in Figure 4.1. The patches of CTAB admicelles were reproducibly and clearly observed. As shown in a height scale, *light shading* is equivalent to a high-level region; on the other hand, *dark shading* is equivalent to a low-level region. The thickness measured directly from the image is just apparently relative thickness. It is not true thickness, because the image is created from long-range interactions between the tip probe and a mica surface in an aqueous solution, thus the tip probe is flown over a mica surface rather far away. Accordingly, the obtained image was the image of “long-range force field” of sample surface.

To measure a true thickness, dark (labeled 1) and lights shading (labeled 2) regions, were characterized as shown in Figure 4.2. The method to measure the thickness of CTAB admicelles closely followed Ceotto *et al.* [26]. Only approaching lines (upper lines in Figure 4.2) were needed for the measurement of admicelle

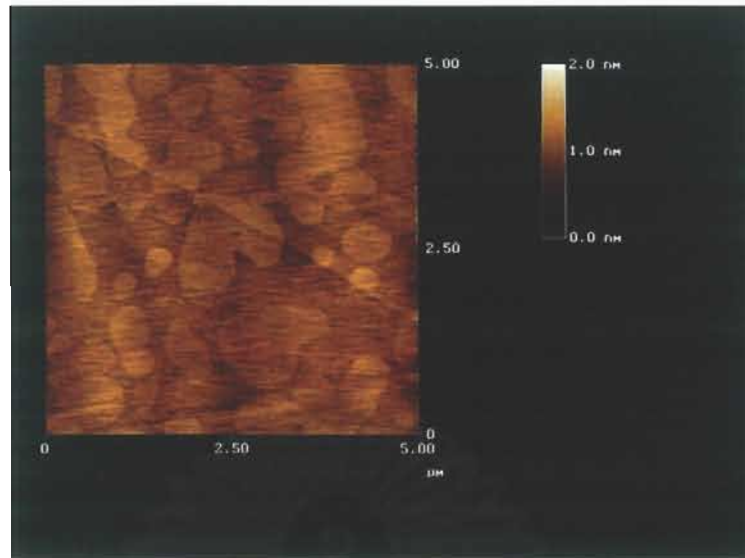


Figure 4.1: Topographic image of CTAB admicelles on a mica surface in the 700 μM CTAB aqueous solution and 3 hours equilibration.

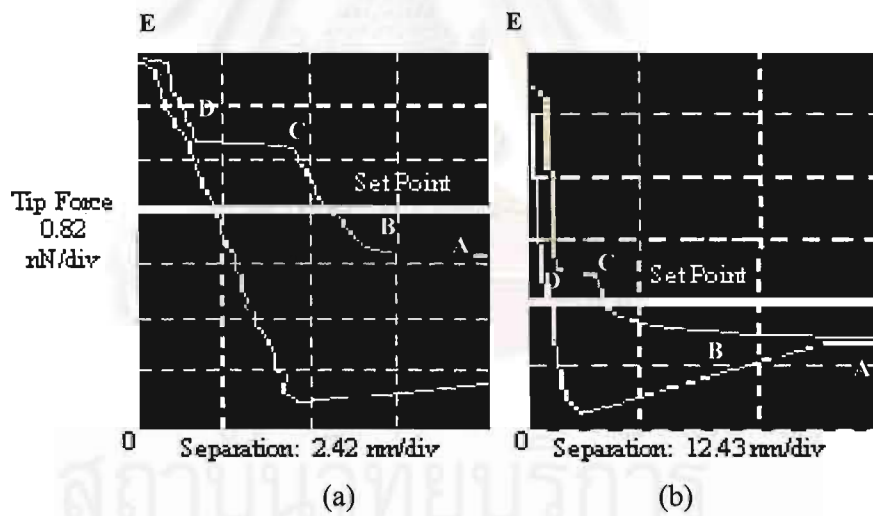


Figure 4.2: The force-versus-separation curves of CTAB (a) *monolayer* (dark region: block 1) and (b) *bilayer admicelle* (light region: block 2) adsorbing on a mica surface in the 700 μM CTAB aqueous solution of Figure 4.1. Upper line and lower line represent the curves for the probing approached and drawn-off probe, respectively.

thickness. On the approaching of the tip probe downward to the sample surface, the tip probe moving from a position far away from the surface (point A), the tip probe senses no force at this position. Until a certain position (point B), the tip probe begins sensing a repulsive force from the surface due to a long-range electrical double layer interaction between the tip probe and the surface. The force gradually increases during the tip probe approaching the surface until the tip probe firstly touches the surface of admicelles (point C). Instantly, the tip probe is attracted downward to the surface due to the attractive van der Waals and consequent hydrophobic force between CTAB hydrophobic chains of adsorbed CTAB on mica surface and the tip probe surface resulting in an instant penetration of the tip probe through the admicelles vertically. This penetration results the tip probe instantly moves downward at almost constant force from point C to point D until it touches mica surface at point D. The distance between point C and D is interpreted as the true thickness of surface layers, i.e., monolayer and bilayer admicelles. Thus, the measured thicknesses are determined as 2.3 and 4.2 nm for the dark and light shading regions, respectively [26]. According to Campanelli and Scaramuzza, the fully extended molecular length of CTAB is 2.16 nm. It means that the measured thicknesses are approximately one and two folds of such CTAB length, respectively [28]. By thickness comparison, this implies that the dark shading region is CTAB monolayers, whereas the light shading regions are bilayer admicelles. The admicelle-covered area was more than 85%. Therefore, the force-separation curve confirmed the existence of the CTAB bilayer admicelles. The simple presentation of monolayer and bilayer admicelles adsorbed on hydrophilic surface of mica is shown in Figure 4.3. The bilayer admicelle generally provides two different adsorption sites for adsorbates, i.e., palisade layer and hydrophobic core. The existence of bilayer admicelles can act as a microreactor where the palisade layer prefers less non-polar component such as TEOS while the hydrophobic core for non-polar one such as TBOS.

After point D, the tip probe is continuously pressed by a cantilever moving for a short distance until the force is high enough at a certain value at point E. Then the probe begins drawing off until it reaches the beginning point A again (lower line). The force-versus-separation curves after point D have no meaning for the thickness measurement of admicelles.

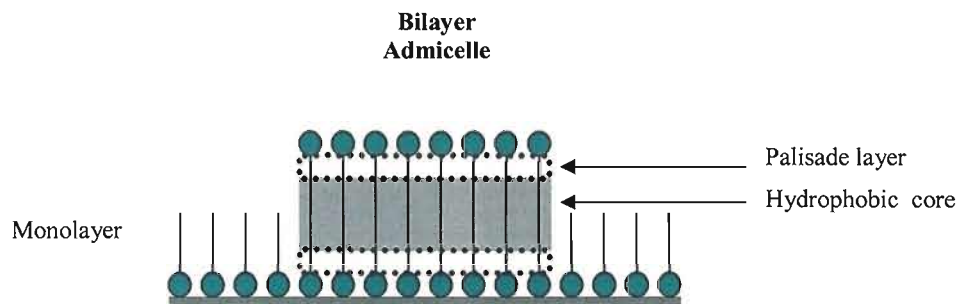


Figure 4.3: A simple representation of monolayer and bilayer admicelle adsorbed on a hydrophilic surface of mica. The admicelle provides two different adsolubilization sites for adsolubilizates, i.e., palisade layer and hydrophobic core.

4.1.2 Adsorption of TBOS (without CTAB)

In the absence of CTAB and the equilibration time was varied from 20 minutes to 24 hours, the results show that TBOS initially adsorbs as single short cylindrical aggregates (Figure 4.4(a)) randomly distributed on the mica surface. They rapidly become solid and adhere to the mica surface rather strongly, as evidenced by the difficulty in removing them with the AFM tip while scanning with high force. This shows that the polymerization reaction of TBOS in aqueous solution still occurs rapidly in the absence of surfactant. The hydrolysis and condensation reactions of TBOS give silica as a final product chemically linking to the mica surface immediately after TBOS adsorbs on mica surface. The formation of the cylindrical aggregates is expected as TBOS prefers hydrolysis at near neutral pH [29], and the aggregates prefer one-direction growth [30, 31]. At longer adsorption times we found that TBOS adsorbs as pair-wise cylindrical aggregates (one cylinder aligned parallel to another) as shown in Figure 4.4(b). The pair-wise aggregates grow further in three dimensions and form globular clusters (Figures 4.4(c) and (d)). At adsorption times exceeding 24 hours, two surface patterns were observed, i.e., ordered (Figure 4.4(e)) and disordered (Figure 4.4(f)) fibrous textures with some fibers overlapping others. At longer reaction times almost the whole mica surface was covered by the globular aggregates. Growth parallel to the surface plane is restricted. Thus, the aggregates tend to grow outward from the mica surface allowing high aspect ratio fibers to grow towards the aqueous solution (one end links to solid surface, another end points outward mica surface). We initially thought that these fiber chains were driven to one direction by rinsing the mica surface with water and methanol in one direction,

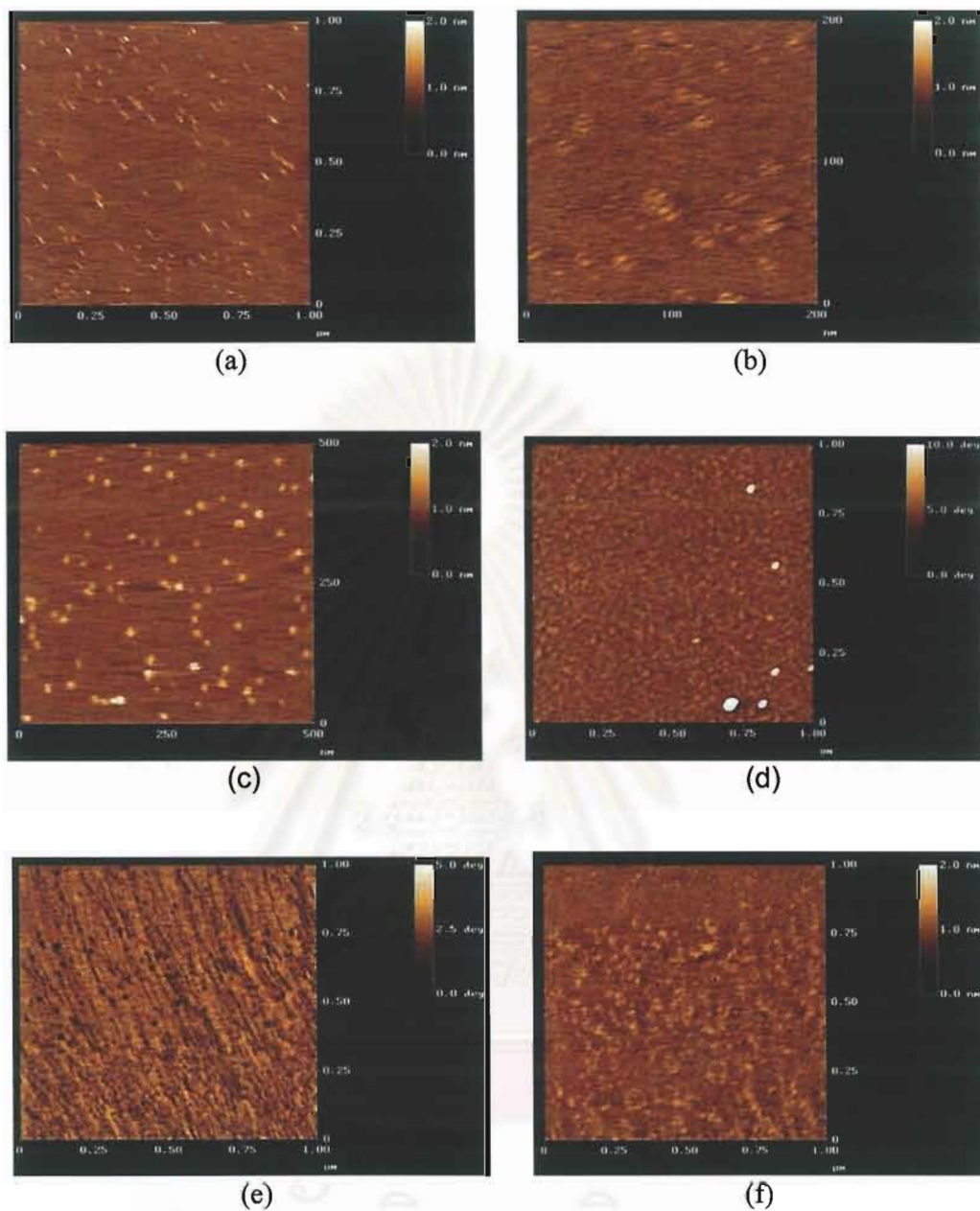


Figure 4.4: Images of mica surface modified by the $0.0266 \mu\text{M}$ TBOS aqueous solution at various TBOS adsorption (or reaction) times of (a) 20 min (b) 60 min (c) 90 min (d) 2 hr (e) 1 day and (f) 1 day; at different area.

resulting in the ordered / aligned fibers. This phenomenon is similar to polystyrene aligning in one direction on mica surface obtained by rinsing mica surface with polystyrene-containing benzene solution [32]. The disordered fibers may be due to an uneven rinsing process.

4.1.3 Admicellar Polymerization of TBOS

4.1.3.1 Adsolubilization and Film Characterization

The adsolubilization time was 1 hours while the TBOS concentrations were varied from 0- 1.31 μM . The adsolubilization of TBOS existing on the mica surface was observed directly by a contact AFM in the TBOS-CTAB aqueous solution. The results showed that at low TBOS concentrations, a fibrous texture was observed on mica surface as shown in Figure 4.5(b). The fiber-covered area was less than 30%. The fiber sizes range from 80-160 nm in diameter. These observed diameters were much larger than that of a typical CTAB cylindrical admicelle (5-6 nm), implying that the admicelles could swell due to adsolubilization of TBOS or the TBOS phase separated within the admicelle [33, 34]. When the TBOS concentration was increased to 0.266 μM , the surface morphology was changed to distributed hemispheres (Figure 4.5(c)) with diameters ranging from 150 to 400 nm, noticeably larger than the fibers. This morphology implies that the TBOS in the admicelle was not distributed according to the initial admicelle structure but rather a new or separate phase. Apparently, the adsolubilization of TBOS could cause phase transitions (or separation) within the adsorbed film. This phase transition leads to small aggregate covering some surface area (about 45-55% coverage). Additionally, it was observed that these fibers and hemispheres are soft. They could be mechanically removed by the AFM tip and would then “self-repair”. Nevertheless, they are stable as soft structures for a long time (more than 6 hours). Therefore, it could be concluded that the fibers and hemispheres was TBOS molecules encapsulated within the CTAB monolayer in the same manner as a microemulsion or macroemulsion and was stabilized by surfactants. This monolayer inhibited TBOS from water exposure and thus retarded the polymerization reaction. This phenomenon is similar to n-alkoxysilane emulsion stabilized by surfactant adsorption at emulsion-water interface as reported by Fisher [10].

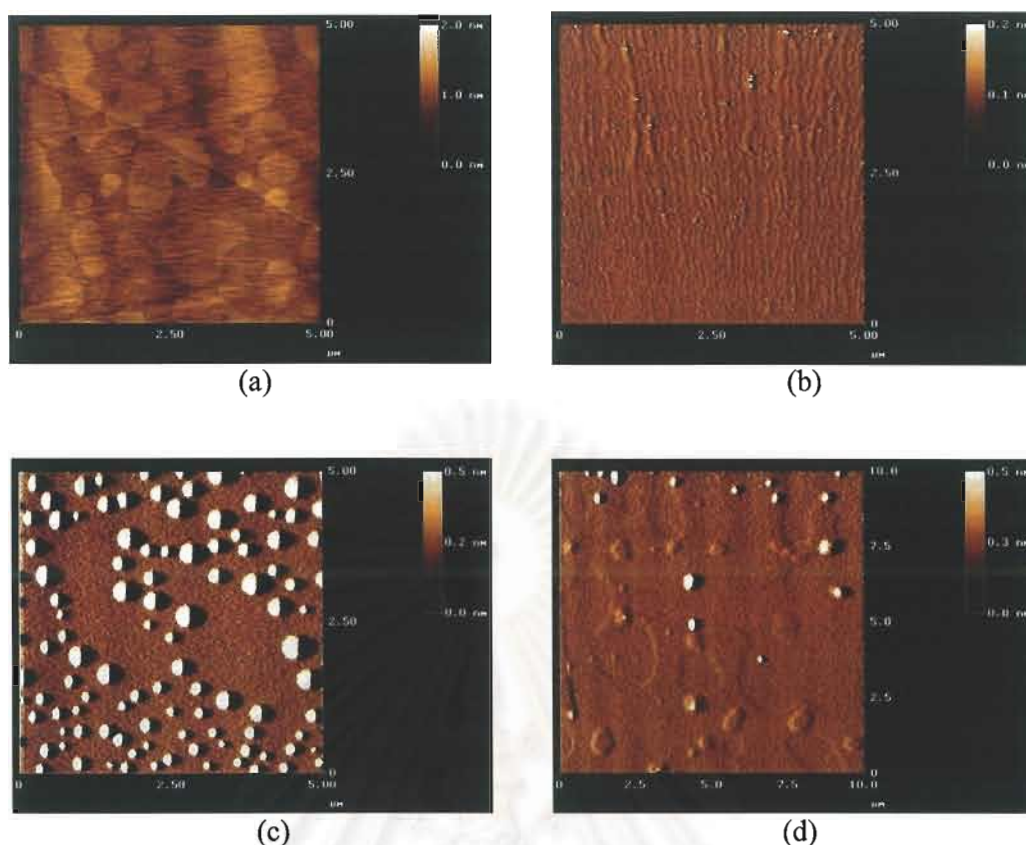


Figure 4.5: Topographic images of mica surfaces covered by the TBOS-CTAB adsorbed aggregates directly imaged by the contact mode AFM in the aqueous solutions of 700 μM CTAB and (a) 0 μM TBOS (b) 0.0266 μM TBOS (c) 0.266 μM TBOS and (d) 1.31 μM TBOS at adsorption/reaction time of 1 hour.

At higher TBOS concentration, 1.31 μM , flat layers or multilayer (Figure 4.5(d)) were observed. The layers were hard to be removed and thus assumed to be solid, three-dimensional structures. They appeared to act as a strong support for second layers or hemisphere growth. At concentrations equal to its water solubility, TBOS possess maximum activity. The amount of silicate anions or oligomers coming from initial hydrolysis and condensation of TBOS in the bulk solution are dominant. These anions possibly solubilize at the admicelle-solution interface. This effect provides lower curvature of the previous hemispheres. The densely adsorbed anions are directly exposed to water and consequently undergo fast hydrolysis and condensation reaction providing flat layers of silica film covered on mica surface as mentioned. This phenomenon increases aggregate-covered area from 20-30% of fibrous textures to 45-55% of flat layers.

It was found that dried silica films with good persistence (after rinsing with water and methanol and then dried at ambient temperature) could be achieved after 24 hours reaction time. Figure 4.6(a) shows that our surfactant removal method cannot remove all adsorbed surfactant molecules from the mica surface as there are some small discrete aggregates of CTAB on mica surface. However it did not disturb the images of silica film topography as shown in Figures 4.6(b)-(d). Figures 4.6(b)-(d) are similar to the ones directly observed in the aqueous solution of CTAB-TBOS at the same composition (Figure 4.5(b)-(d)). It means that (1) structure of film may not change with time and (2) dewetting during film drying does not affect final film structure.

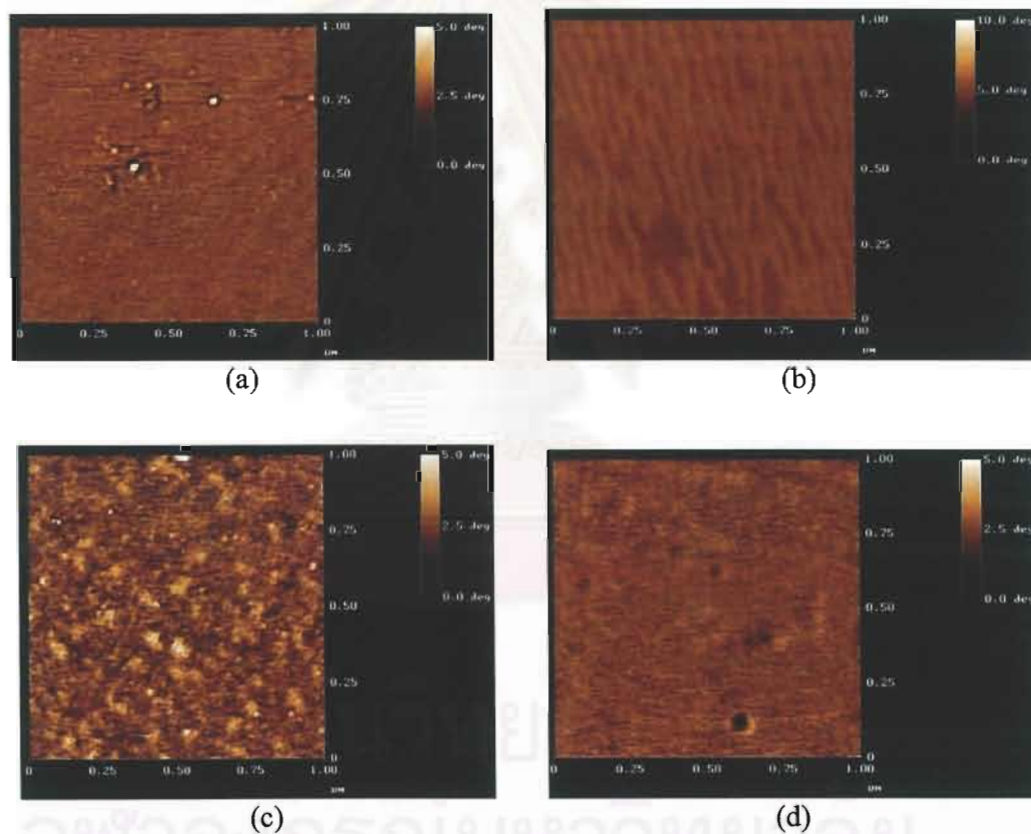


Figure 4.6: Topographic images of mica surfaces covered by silica films imaged by the tapping mode AFM in air after surface-modified in the aqueous solutions of 700 μM CTAB and (a) 0 μM TBOS (b) 0.0266 μM TBOS (c) 0.266 μM TBOS and (d) 1.31 μM TBOS for 24 hour and then dried.

4.2 Silica Film Formation in Triton X-100/TEOS/Styrene-AIBN System

4.2.1 Adsorption of TEOS

In Figure 4.7, the tapping mode AFM reveals both topographic and phase images simultaneously of the dried silica film formed on the mica surface obtained from the 3.0 μM TEOS aqueous solution in the absence of triton X-100. The film did not clearly exist. A small number of silica particles were found randomly dispersed across the mica surface with narrow size distribution. TEOS cannot adsorb and further nucleate well on the mica surface because TEOS is rapidly hydrolyzed and then subsequently condenses to form small silicate anions, which possess negative charges the same as mica [29]. Therefore, the film was barely formed and observed on the mica surface.

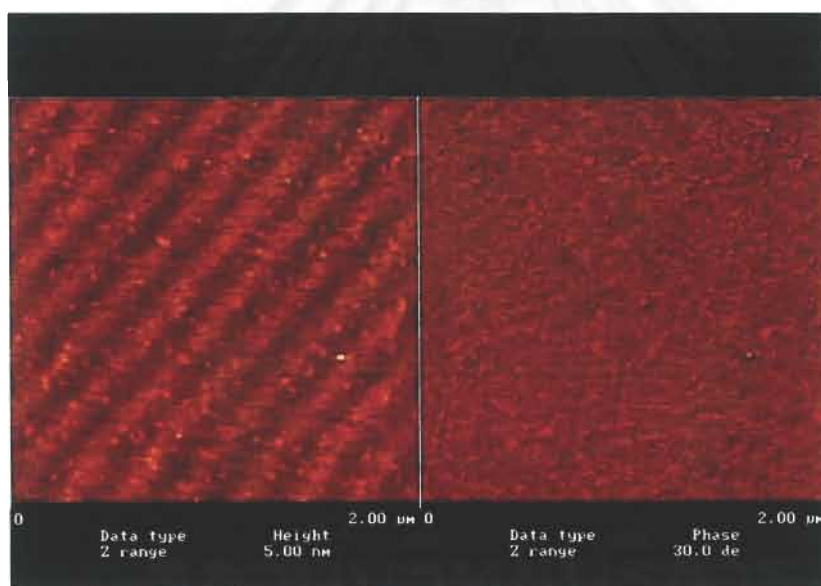


Figure 4.7 Topographic and phase images of the silica film formed on the mica surface in the 3.0 μM TEOS aqueous solution in the absence of triton X-100.

It was noted that a sine-wave pattern in surface topographic image originated from light reflection from mica surface observed during imaging always disturbs the true image. The phenomenon was observed in almost topographic images and was ignored.

In the presence of 0.2 mM triton X-100 ($\text{cmc} = 0.23 \text{ mM}$), at which it adsorbs as two dimensional aggregates, admicelles [27]. the surface morphology of silica film on the mica surface exhibits the thin homogeneous globular-shaped features and smooth with well-connected silica particles thorough the mica surface (Figure 4.8). This implies that triton X-100 admicelles dominantly promote the adsorption/solubilization of TEOS at the admicelle-water interface.

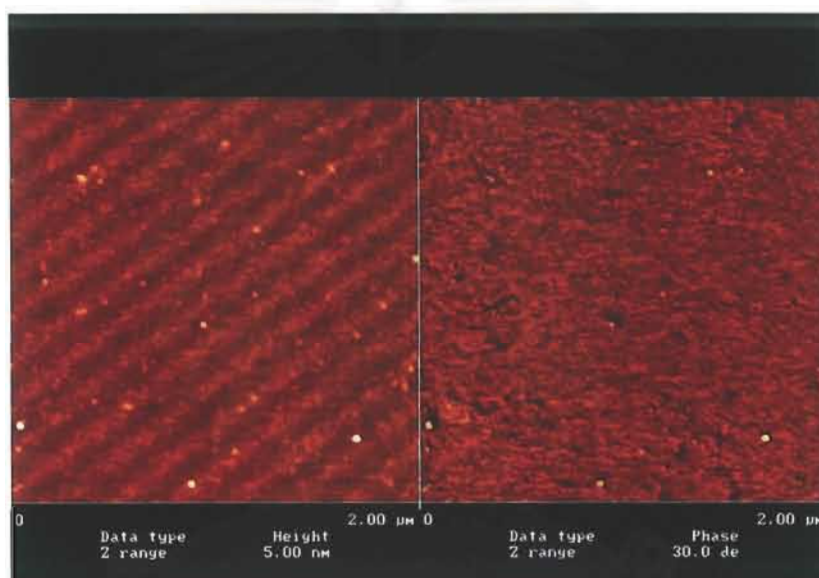


Figure 4.8 Topographic and phase images of the silica film formed on the mica surface in the $3.0 \mu\text{M}$ TEOS- 0.2 mM triton X-100 aqueous solution.

4.2.2 Polystyrene Film Formation

In the absence of triton X-100, the image observed was lack of clear feature (very flat topography), when mica was exposed in the aqueous solution of styrene (0.3 and $3.0 \mu\text{M}$) and AIBN initiator (0.05 and $0.5 \mu\text{M}$ respectively) at 80°C as shown in Figure 4.9. It was indicated that there was no significant formation of polystyrene aggregates on the mica surface. However, large polystyrene particles were observed, it could be the polystyrene particles from polymerization in the bulk depositing onto the

mica surface but did not significantly effect the surface morphology. The obtained surface coverage was about 20%. It has been reported that styrene generally polymerizes effectively in the presence of the AIBN initiator in an aqueous environment at moderate temperature of 80°C but it cannot adsorb well on the mica surface [35].

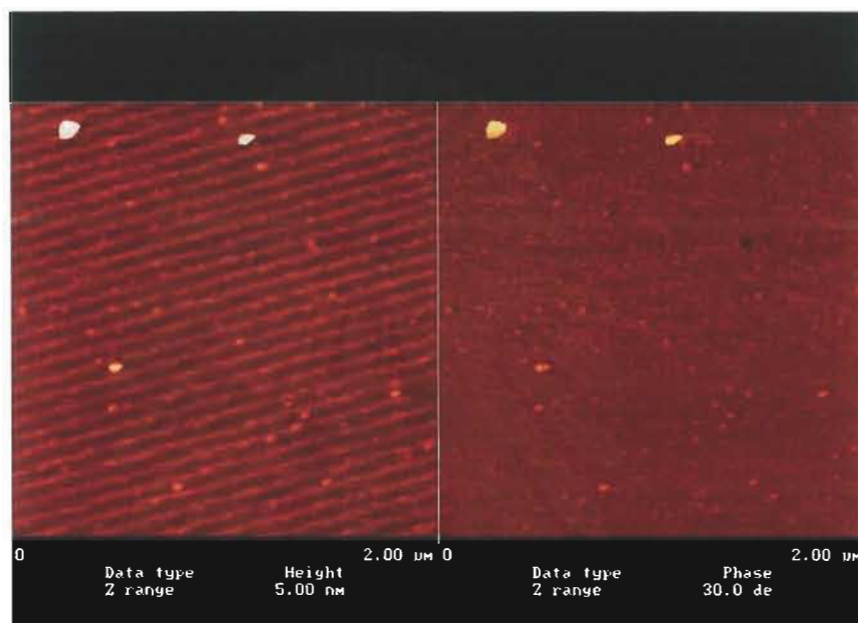


Figure 4.9 Topographic and phase images of the polystyrene film formed on the mica surface in the 3.0 μM styrene-0.5 μM AIBN aqueous solution.

In the presence of triton X-100 (0.2 mM), the topographic image showed high contrast, which revealed the existence of polystyrene droplets on the mica surface. At low styrene loading (0.3 μM) showed smooth and homogeneous surface indicating that styrene concentration was sufficient to adsorb without phase separation. The features at high styrene loading (3.0 μM) were predominantly discrete polystyrene droplets and/or clusters that appeared to have nucleated at many sites. Surface coverage increases dramatically leading to the conclusion that triton X-100 admicelle effectively solubilizes styrene and AIBN. Since the initial styrene monomer concentration (3.0 μM) is higher than the saturation concentration in the admicelle, the excess of monomer in the bulk solution occurs phase separation forming droplet-like aggregates upon polymerization. Both polystyrene in the admicelle and in the

bulk as the droplets can deposit on the mica surface during washing and drying as observed in Figure 4.10.

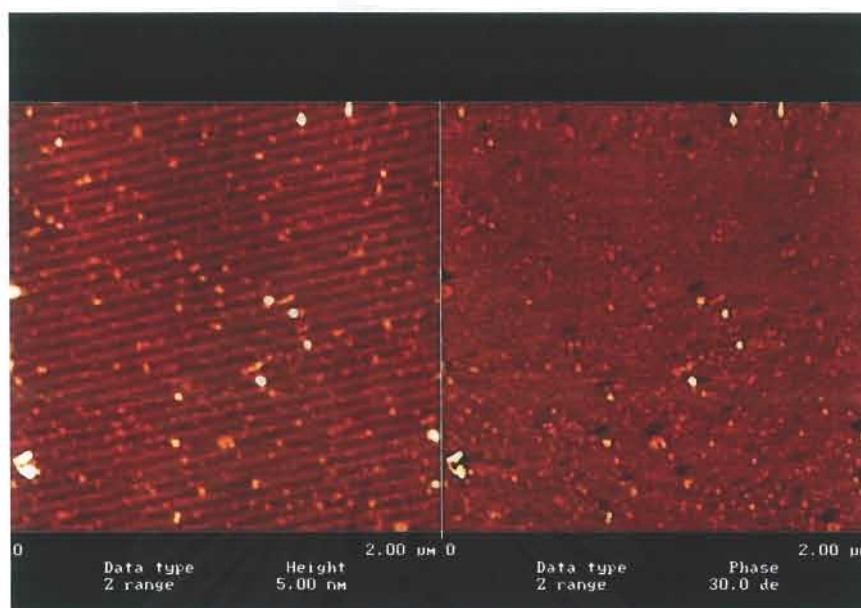


Figure 4.10 Topographic and phase images of the polystyrene film formed on the mica surface in the 3 μM styrene-0.5 μM AIBN-0.2 mM triton X-100 aqueous solution.

4.2.3 Admicellar Polymerization of TEOS/ Styrene-AIBN

In the absence of triton X-100, styrene (0.3 μM and 3.0 μM) and AIBN were introduced into a TEOS (0.3 μM and 3.0 μM) aqueous solution as surface modifying solution, a number of loosely packing discrete aggregates were observed scattering across the mica surface as shown in Figure 4.11. The aggregates are difficult to remove from the mica surface by solvent rinsing and appear to be narrow in size distribution. Both surface coverage and morphology is rather independent of TEOS and styrene concentrations in the concentration range we performed. The observed surface coverage is low (about 10%); however, it is a bit higher than that observed on the mica surface modified in the aqueous solution of TEOS (Figure 4.7) and styrene (Figure 4.9) individually. These means that styrene does not promote TEOS adsorption significantly without the presence of surfactant.

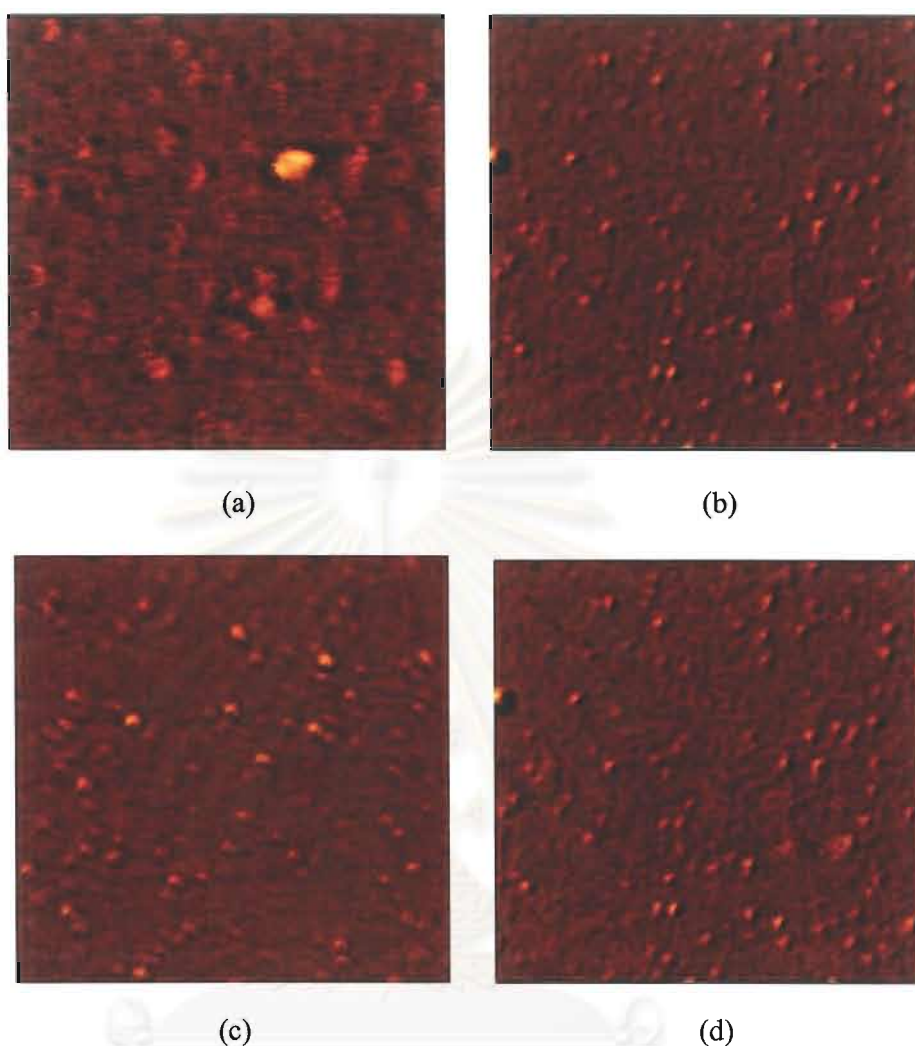


Figure 4.11: 500 nm x 500 nm AFM image of the polystyrene/silica discrete film formed on the mica surface in the aqueous solution of (a) 3.0 μM TEOS+3 μM styrene (b) 0.3 μM TEOS+3.0 μM styrene (c) 3.0 μM TEOS+0.3 μM styrene and (d) 0.3 μM TEOS+0.3 μM styrene with the presence of AIBN (styrene: AIBN = 6:1).

In the presence of triton X-100, which it adsorbs as two dimensional aggregates, admicelles [27], the concentrations of styrene and TEOS were varied (0.3 μM to 3.0 μM). The results show that the presence of admicelles dramatically alters the surface morphology of polystyrene/silica films on the mica surface as shown in Figure 4.12. The results demonstrated that the surface morphology of the film depends on the

amount of styrene and TEOS feed concentrations. The surface morphology of the lower styrene and TEOS concentrations exhibits deep valleys, less compact and less dense structures. Figure 4.12(a) shows the image of the polystyrene/silica aggregate formed on the mica surface in the aqueous solution of 3.0 μM TEOS together with 3.0 μM styrene in the presence of AIBN (styrene: AIBN = 6:1) and triton X-100. As the styrene concentration increases from 0.3 μM to 3.0 μM , the packing of domains (periodic structures or aggregates) becomes homogeneous surface structure. Higher concentration of styrene assisted the incorporation of TEOS in the polystyrene matrix, inhibited the formation of silica particles on the surface. This composition provided surface coverage reaching 100%, thicker, denser, and higher compact with well-connected periodic structure comparing with the silica film from TEOS (Figure 4.8) and polystyrene from styrene and AIBN (Figure 4.10) with the presence of triton X-100. The multiple scans of the surfaces in many different locations did not detect the presence of multiple layers of material or any surface unevenness. These results confirmed that the formed composite films completely and uniformly coat (100% coverage) the mica surface. This implies that triton X-100 admicelles promote the deposition of the silica aggregates. Also, styrene and TEOS synergistically improve that deposition and the adhesion between the film and the mica surface.

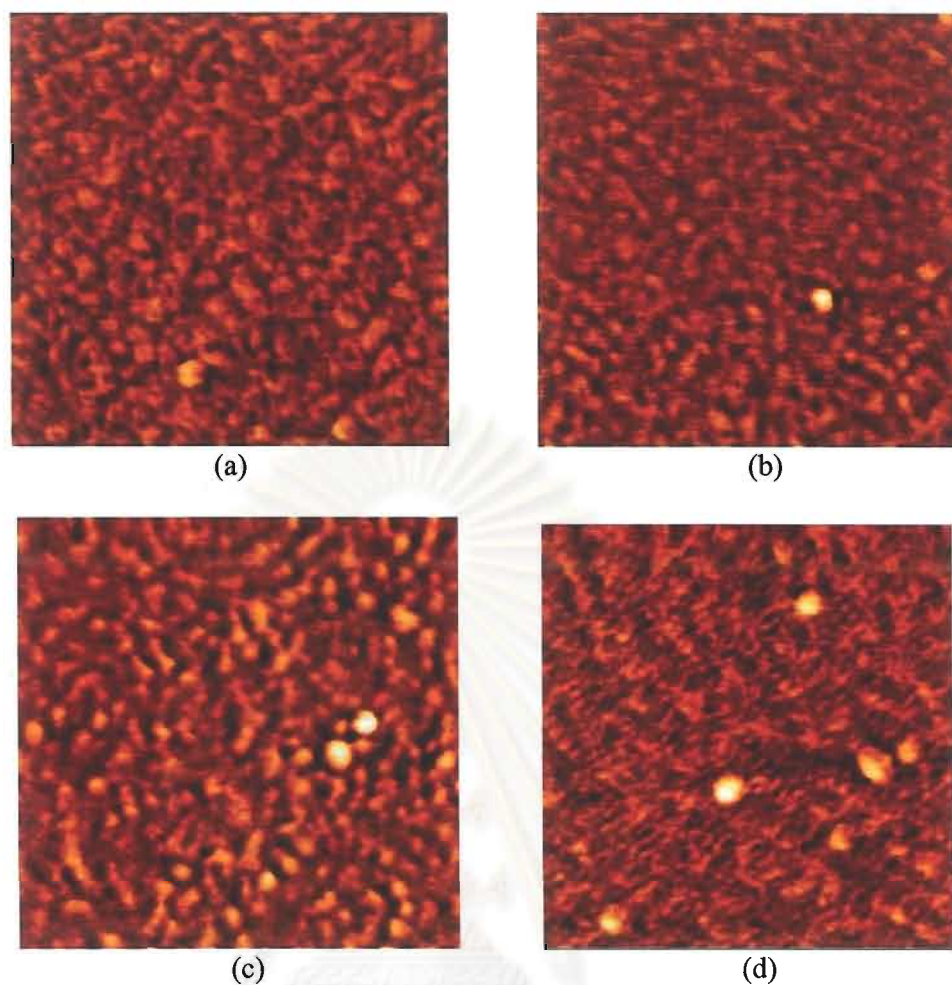


Figure 4.12: 500 nm x 500 nm AFM image of formed polystyrene/silica composite aggregate on a mica surface in the aqueous solution of (a) 3.0 μM TEOS+3.0 μM styrene (b) 0.3 μM TEOS+3.0 μM styrene (c) 3.0 μM TEOS+0.3 μM styrene and (d) 0.3 μM TEOS+0.3 μM styrene with the presence of initiator AIBN (styrene: AIBN = 6:1) and 0.2 mM triton X-100.

สถาบันวิทยบริการ
จุฬาลงกรณ์มหาวิทยาลัย



Chapter 5

Conclusions

The admicellar polymerization of silica precursors, TBOS in admicelle of CTAB was studied. TBOS was initially proposed as an appropriate hydrophobic silica precursor because of its slow kinetic reaction rate with water and less water-soluble which prefers solubilization in admicelle core. The topographic images showed fibers, hemispheres and flat layers exist along with the surface coverage increasing on the mica surface as the TBOS feed concentration was increased. The results showed phase separation at low TBOS concentration. At high TBOS concentration, where there was no phase separation, the silica film, flat layer or multilayer was possibly from solubilization of silicate anion or oligomers at the admicelle-solution interface and the silica film coverage reached maximum at 55% compared to maximum coverage of the admicelle observed (85%).

Due to the limitation of TBOS solubility, a possible way to increase silica film coverage is to change silica precursor from TBOS to TEOS; however, TEOS is more polar and more dissolvable in water. Nevertheless, TEOS is easily hydrolyzed and condensed (partial polymerized) in an aqueous environment, the polymerized products (e.g. silicate anions or oligomers), which are able to dissolve in water much better than TEOS, will adsorb at admicelle-water interface preferentially [29, 13].

Wu *et al.* (1987) demonstrated organic monomers that adsorb into the admicelle interior sharing the hydrophobic interaction with the amphiphile tails (Wu *et al.*, 1987). O'Haver *et al.* (1995) demonstrates admicellar polymerization reaction of styrene and the monomer in the bulk solution begin to re-equilibrate by diffusing into the admicelle. Furthermore, work done by Jang and Park (2002), polystyrene-silica hybrid materials from styrene and tetraethyl orthosilicate (TEOS) in the presence of silane-coupling agent, 3-(trimethoxysilyl)-propyl-methacrylate (MPS) was successfully prepared by an *in-situ* sol-gel process. Triethoxysilyl group can be incorporated into polystyrene as side chains by the free-radical copolymerization of polystyrene with silane-coupling agents, and simultaneously polystyrene-silica hybrid materials with covalent bond between two phases were formed via the sol-gel

reaction. Thus, we proposed addition of styrene monomer to assist adsolubilization of TEOS and AIBN as a polymerization initiator at moderate temperature.

Accordingly, triton X-100 was chosen as surfactant instead of CTAB because it possesses a large hydrophilic head group (9-10 EO groups), much larger than CTAB head group [36], which can provide much larger hydrophilic space in admicelles for adsolubilizing TEOS and its polymerized products.

The composite films of styrene-AIBN and TEOS formed in the absence of surfactant showed that the surface morphology of the film on mica was independent of the styrene and TEOS feed concentrations. The surface morphology illustrated multigranular features scattered across the mica surface, which appeared to be governed by the presence of TEOS but not by the presence of styrene.

For the films systems in the presence of triton X-100 the surface morphology was dramatically altered by the styrene and TEOS feed concentrations. The packing of domains and aggregates of the resulting samples become more densely packed and homogeneous as the styrene or TEOS feed concentration increased. As the results, the surface aggregates also grow larger, and consequently the surface coverage is increased. Well-defined spherical particles were clearly observed at low TEOS concentrations incorporated into the styrene matrix polymer leading to higher heterogeneity. This type of particles disappeared at the styrene and TEOS concentrations of 3 and 3 μM , respectively. This implies that higher concentration of styrene assisted the incorporation of TEOS in the polystyrene matrix, inhibited the formation of silica particles on the surface.

It was clearly found that styrene at the concentration of 3 μM and TEOS at the concentration of 3 μM synergistically produced a polystyrene/silica composite film that was dense, highly compact with well-connected with periodic structure. Moreover, vacant or empty space and loose aggregate were not present.

Recommendations

The results of this research have shown that formation of silica thin film on mica surface can be done through admicellar polymerization of inorganic silica precursor. It opens the opportunity to fabricate the organic/inorganic composite film on mica by surfactant template technique with fewer chemicals used. This approach provides an

attractive alternative to the processing of films, especially in applications where substrates cannot be exposed to high temperatures. Further study is recommended to investigate different type of substrates, the properties of thin film material in terms of the synthesis conditions such as effect of pH, styrene and TEOS concentrations and optimization conditions to achieve the best properties of the silica film.

Comments and Remarks

1. SEM and TEM are not sensitive enough to detect the changes on a mica surface because low resolution and special sample preparation and imaging environment.
2. XRD and FTIR are not sensitive enough to detect the changes on a mica surface because of interference from background (mica).
3. Glass surface is highly rough. The roughness disturbs the true surface topography of admicelles during AFM tip scanning.



References

1. J.H. O'Haver, J.H. Harwell, L.L. Lobbance and E.A. O'Rear III, Adsolubilization, Solubilization in Surfactant Aggregates, Marcel Dekker, New York (1995).
2. P. Kekicheff, H.K. Christenson and B.W. Ninham, Adsorption of cetyltrimethylammonium bromide to mica surface below the critical micellar concentration, Colloids and Surfaces 40, 31-41 (1989).
3. L. Grosse and K. Estel, Thin surfactant layers at solid interface, Colloid and Polymer Science 278, 1000-1006 (2000).
4. J. Dickson and J.H. O'Haver, Adsolubilization of naphthalene and α -naphthol in C_n TAB admicelles, Langmuir 18, 9171-9176 (2002).
5. K. Esumi, N. Watanabe and K. Meguro, Polymerization of styrene adsolubilized in polymerizable surfactant bilayer on alumina, Langmuir 7, 1775-1778 (1991).
6. S.S. Sakhalkar and D.E. Hirt, Admicellar polymerization of polystyrene on glass fibers, Langmuir 11, 3369-3373 (1995).
7. G.P. Funkhouser, M.P. Arevalo, D.T. Glatzhofer and E.A. O'Rear, Solubilization and adsolubilization of pyrrole by sodium dodecyl sulfate: polypyrrole formation on alumina surfaces, Langmuir 11, 1443-1447 (1995).
8. K. Esumi, K. Mizuno and Y. Yamanaka, Adsolubilization behavior of 2-naphthol into adsorbed anionic surfactant and poly(vinylpyrrolidone) at an alumina/water interface, Langmuir 11, 1571-1575 (1995).
9. C.L. Lai, J.H. Harwell, E.A. O'Rear, S. Komatsuzaki, J. Arai, T. Nakakawaji and Y. Ito, Formation of poly(tetrafluoroethylene) thin films on alumina by admicellar polymerization, Langmuir 11, 905-911 (1995).
10. P.D. Fisher, Stable aqueous emulsions of nonpolar silanes having constant particle size, International Publication No. WO 00/34207 (2000).
11. T.M. Meada, Hydrolysable silane emulsions and method for preparing International Publication No. WO 01/00309 A1 (2001).
12. S. Vancheeswaran, R.U. Halden, K.J. Williamson, J.D. Ingle. Jr. and L. Semprini, Abiotic and biological transformation of tetraalkoxysilanes and trichloroethene cometabolism driven by tetrabutoxysilane-degrading

- microorganisms, Environmental Science and Technology, 33, 1077-1085 (1999).
13. M.J. Rosen, Surfactants and interfacial phenomena, 2nd Edition: New York: John Wiley & Sons (1988).
 14. R.E. Klein, Sol-Gel Technology for Thin Films, Fibers, Preforms, Electronics, Electronics, and Specialty Shapes, 1sted, New Jersey: Noyes Publications (1988).
 15. M. Kimura, K. Wada, K. Ohka, K. Hanabusa, H. Shirai and N. Kobayashi, Organic-inorganic composites comprised of ordered stacks of amphiphilic molecular disks, The Journal of American Chemical Society, 123, 2438-2439 (2001).
 16. R. Tamahi and Y. Chujo, Synthesis of polystyrene and silica gel polymer hybrids utilizing ionic interactions, Chemistry of Materials, 11, 1719-1726 (1999).
 17. S. Reculosa, C. Poncet-Legrand, S. Ravaine, C. Mingotaud, E. Duguet and E. Bouegeat-Lami, Syntheses of raspberry-like silica/polystyrene materials, Chemistry of Materials, 13, 3002-3007 (2002).
 18. J. Wu, J.H. Harwell and E.A. O'Rear, Two-dimensional reaction solvents: surfactant bilayers in the formation of ultrathin films, Langmuir, 3, 531-537 (1987).
 19. S.S. Sakhalkar and D.E. Hirt, Admicellar polymerization of polystyrene on glass fibers, Langmuir, 11, 3369-3373 (1995).
 20. R.K. Iler, The Chemistry of Silica, New York: John Wiley and Sons (1979).
 21. J. Penfold, E. Staples and I. Tucker, On the consequence of surface treatment on the adsorption of nonionic surfactants at the hydrophilic silica-solution interface, Langmuir, 18, 2967-2970 (2002).
 22. H.N. Skoog, F.J. Holler and T.A. Nieman, Principle of Instrumental Analysis, 5th ed.; Singapore, Tomson Learning (1998).
 23. M.A. Osman, G. Seyfang and U.W. Suter, Two-dimensional melting of alkane monolayer ionically bonded to mica, The Journal of Physical Chemistry B, 104, 4433-4439 (1994).

24. J. Narkiewicz-Michalek, A theoretical interpretation of cationic surfactant adsorption on mica, monitored by electron spectroscopy for chemical analysis: Effects of the surface energetic heterogeneity of mica, Langmuir, 8, 7-13 (1992).
25. W. Cantrell, and G.E. Ewing, Thin film water on muscovite mica, The Journal of Physical Chemistry B, 105, 5434-5439 (2001).
26. G. Ceotto, E.F. Souza and O. Teschke, Ionic surfactant films imaged by atomic force microscopy, J. Molecular Catalysis A: Chemical, 167, 225-233 (2001).
27. J. Zhao and W. Brown, Comparative study of the adsorption of nonionic surfactants: triton X-100 and C₁₂E₇ on polystyrene latex particles using dynamic light scattering and adsorption isotherm measurements, The Journal of Physical Chemistry, 100(9), 3775-3782 (1996).
28. A.R. Campanelli and L. Scaramuzza, Hexadecyltrimethylammonium bromide, Acta Crystallographica C: Crystal Structure Communications, 42, 1380-1383 (1986).
29. H.D. Gesser and P.C. Goswami, Aerogels and related porous materials, Chemical Reviews, 89, 765-788 (1989).
30. K.L. Chopra, Thin Film Phenomena, McGraw-Hill, New York (1969).
31. F. Kleitz, F. Marlow, G.D. Stucky and F. Schuth, Mesoporous silica fibers: synthesis, internal structure, and growth kinetics, Chemistry of Materials, 13, 3587-3595 (2001).
32. O. Karthaus, K. Ijiri and M. Shimomura, Ordered self-assembly of nanosize polystyrene aggregates on mica, Chemistry Letters, 25, 821-822 (1996).
33. J.F. Liu and W.A. Ducker, Surface-induced phase behavior of alkyltrimethylammonium bromide surfactants adsorbed to mica, silica, and graphite, J. Physical Chemistry B, 103, 8558-8567 (1999).
34. W.A. Ducker and W.J. Wanless, Adsorption of hexadecyltrimethylammonium bromide to mica: nanometer-scale study of binding-site competition effects, Langmuir, 15, 160-168 (1999).
35. R. Saechia, Atomic force microscope studies of the ultrathin polystyrene/silica composite film formation on mica, M.S. Thesis, The Petroleum and

- Petrochemical College, Chulalongkorn University (2002).
36. H.Z. Yuan, S. Zhao, G.Z. Cheng, L. Zhang, X. Miao, S.Z. Mao, J.Y. Yu, L.F. Shen and Y.R. Du, Mixed Micelles of Triton X-100 and Cetyl Trimethylammonium Bromide in Aqueous Solution Studied by ^1H NMR, The Journal of Physical Chemistry B, 105(20, 4611-4615 (2001).

